EXHIBIT 2

ed structure is applicable for the crystal structure. Helix VII is two residues shorter and is shifted 10 residues toward the NH_2-terminal, compared to the helix predicted. A zinc atom was close to the molecular surface in a nuclear-coded subunit Vb on the matrix side. The magnesium site was near Cu_A at the interface of subunits I and II. The electron transfer path within the enzyme has essentially been established recently after long and extensive efforts as follows: cytochrome c → Cu_A → heme a → the O_2 binding sites, which includes heme a_3 and Cu_B (*13*). The location of Cu_A seems consistent with its role as the initial electron acceptor from cytochrome c. However, this overall location of the metal site does not exclude the possibility for a direct electron transfer from Cu_A to the heme a_3–Cu_B site.

Structures of two hemes and Cu_B sites. Both heme planes were essentially perpendicular to the membrane plane facing each other at an angle of 104°. Heme a was coordinated with two imidazoles of histidine residues (His^{61} in helix II and His^{378} in helix X). The fifth ligand of heme a_3 was an imidazole of His^{376} in helix X, whereas Cu_B was coordinated by three imidazoles of His^{240} in helix VI and His^{290} and His^{291}, both in a nonhelical fragment between helices VII and VIII. These ligations are consistent with those proposed as a result of mutagenesis experiments (*12*). The heme a_3 plane was positioned so that the pyrrole ring with a hydroxyfarnesylethyl side chain and the one with a vinyl side group were placed at lower right and left sides, respectively, when viewed from the Cu_B side, with the cytosolic side being considered as the upside. Thus, the pyrrole with methyl and propionic acid groups was located at the upper left side and the one with a formyl and propionic acid groups was located at the upper right. In the case of heme a, the pyrrole with a hydroxyfarnesylethyl side chain was at the lower left, viewed from the Cu_B side (Fig. 2). The hydroxyfarnesylethyl group of heme a was almost in the extended conformation, held by helices I, II, X, XI, and XII, and that of heme a_3 was twisted to

Table 2. Collection of data and statistics of phase determination. The crystals diffracted x-rays up to 2.6 Å resolution. The crystal of the enzyme belongs to the orthorhombic space group of $P2_12_12_1$ with unit cell dimensions a = 189.1 Å, b = 210.5 Å, and c = 178.6 Å, containing two molecules in an asymmetric unit. Intensity data were collected with monochromatized x-ray of 1.0 Å at the Photon Factory, Tsukuba, Japan, by means of a modified Weissenberg camera for macromolecules (*24*). Diffraction intensities were processed with the program DENZO (*25*). Searching more than 50 heavy atom derivatives with MAC Science imaging plate detector (DIP2000) on a Rigaku rotating anode x-ray generator (RU300), we yielded three derivative data sets available for phase determination. Two of three derivatives were prepared by soaking the crystals in Na_2IrCl_6 solutions at various concentrations. The third was a CH_3HgCl derivative. Heavy atom sites of each derivative were located by solving each difference Patterson function at 5 Å resolution. The heavy atom parameters of three derivatives were refined with the program MLPHARE (*26*) of the CCP4 program package. In that MIR (*27*) phase information was poor beyond 5 Å resolution, phases were extended from 5 to 2.8 Å in 200 small steps with the use of solvent flattening (*28*) by means of the program DM of CCP4. The protein mask during the phase extension was determined by the Wang method (*28*) with a sphere of 10 Å and 70 percent solvent content by volume. A free R factor (*29*) for 5 percent of the reflections in each shell was reduced from 0.53 to 0.28. The noncrystallographic symmetry relation between two molecules in an asymmetric unit was determined, and the correlation coefficient $\{\Sigma(\rho1 - \langle\rho1\rangle)(\rho2 - \langle\rho2\rangle)/\Sigma[(\rho1 - \langle\rho1\rangle)^2(\rho2 - \langle\rho2\rangle)^2]^{1/2}\}$ was as high as 0.78. The phase refinement procedure including NCS averaging (*30*) was undertaken, starting at 5 to 2.8 Å resolution. The free R factor and the correlation coefficient at the final stage were 0.26 and 0.92, respectively.

	Native	$IrCl_6$(I)	$IrCl_6$(II)	CH_3HgCl
Resolution ranges (Å)*	100–2.8 (2.9–2.8)	100–3.0 (3.2–3.0)	100–3.0 (3.1–3.0)	100–3.0 (3.1–3.0)
Observed reflections	518,054 (24,542)	319,358 (18,599)	381,828 (28,410)	328,484 (15,186)
Independent reflections	159,742 (13,074)	125,036 (11,545)	133,245 (14,008)	127,548 (9,396)
$I/\sigma(I)$	19.5 (2.2)	10.0 (1.4)	21.3 (2.7)	2.4 (1.5)
Averaged redundancy†	3.2 (1.9)	2.6 (1.6)	2.9 (2.0)	2.6 (1.6)
Completeness (‡)	90.1 (74.4)	86.3 (64.5)	93.0 (79.1)	88.3 (65.7)
R_{merge}§	7.8 (29.0)	9.0 (29.6)	6.2 (23.4)	8.5 (28.4)
R_{iso}‖		7.3 (11.6)	5.7 (8.7)	9.0 (11.4)
R_{Cullis}¶		0.90 (0.97)	0.86 (0.97)	0.79 (0.95)
Phasing power#		0.38 (0.18)	0.54 (0.30)	0.74 (0.34)

*Figures in parentheses are given for the highest resolution shells. †Redundancy is the number of observed reflections for each independent reflection. ‡R_{merge}, $\Sigma_h\Sigma_i|I(h,i) - \langle I(h)\rangle|/\Sigma_h\Sigma_i I(h,i)$, where $I(h,i)$ is the intensity value of the i-th measurement of h and $\langle I(h)\rangle$ is the corresponding mean value of $I(h)$ for all i measurements; the summation is over the reflections with $I/\sigma(I)$ larger than 1.0. ‖R_{iso}, $\Sigma||F_{PH} - F_P|/\Sigma F_{PH}$, where F_{PH} and F_P are the derivative and the native structure factor amplitudes, respectively. ¶R_{Cullis}, $\Sigma||F_{PH} - F_P| - F_H(calc)|/\Sigma|F_{PH} - F_P|$, where $F_H(calc)$ is the calculated heavy atom structure factor. The summation is over the centric reflections only. #Phasing power is root-mean-square (rms) isomorphous difference divided by rms residual lack of closure.

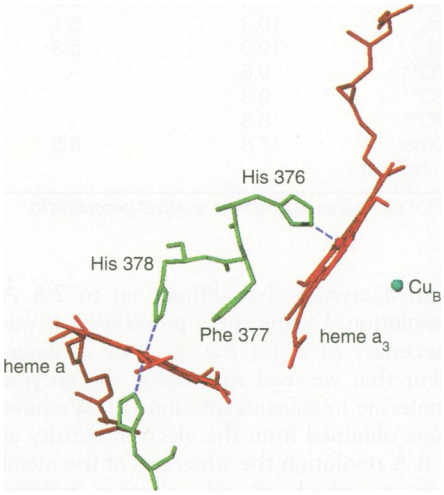

Fig. 3. Structural relation between two hemes in the active site of cytochrome c oxidase. Red structures and green structures represent hemes and amino acid residues in subunit I. A blue ball and red balls define the positions of copper and iron atoms, respectively. The hemes a and a_3 are bridged by three successive residues, His^{376}, Phe^{377}, and His^{378} in the helix X.

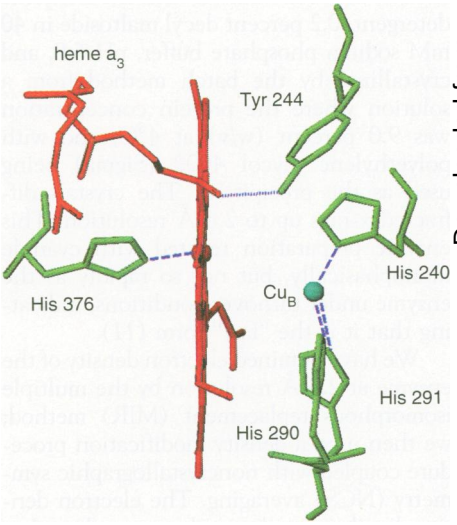

Fig. 4. A side view of the O_2 binding and reduction site. The red structure is heme a_3 and the green ones are amino acids. The dotted line shows a possible hydrogen bond between the hydroxyl of the hydroxyfarnesylethyl group and Tyr^{244}. The broken lines represent coordination bonds. The red and green balls represent the positions of iron and copper atoms, respectively. A close contact between Tyr^{244} and His^{240} with both aromatic rings oriented perpendicular with each other is also shown.

form a U-shaped arm, located between helices VIII and IX. None of the hydroxyfarnesylethyl side chain interacted with the redox centers or the porphyrin aromatic ring system, contrary to the proposals based on the kinetic behavior of the enzyme (*4*, *14*).

A phenyl plane of a phenylalanine (Phe^{377} in helix X) was observed halfway between the two planes of the heme a_3 and one of the imidazole ligands of heme a (His^{378}) (Fig. 3). The distances between the phenyl plane and the two planes on both sides are as short as 3.5 Å. Thus, any change in the orientation and position of the phenyl group, induced by change in the ligation and oxidation state of Fe_{a_3} from the fifth ligand imidazole of His^{376}, adjacent to Phe^{377}, could control the electron transfer between Fe_a and Fe_{a_3}.

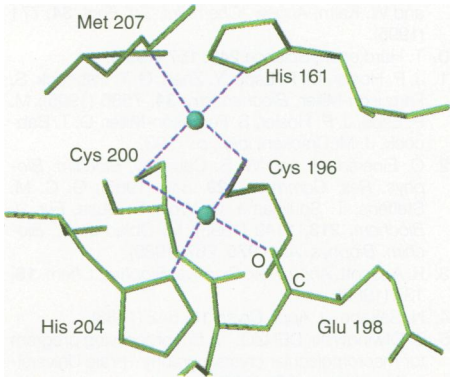

Fig. 5. A representation of Cu_A site showing a [2Cu-2Sγ] structure. Green balls show copper atom positions. Blue broken lines indicate coordination bonds. The peptide carbonyl group of Glu^{198} is illustrated with a bar marked with C and O.

A side view of the heme a_3–Cu_B structure reveals the phenol OH group of tyrosine, Tyr^{244}, in subunit I oriented to the OH of the hydroxyfarnesylethyl group (Fig. 4). The Cu_B site was coordinated only by the three imidazoles of His^{240}, His^{290}, and His^{291}. No other ligand to Cu_B, even water, was detected. The high spin Fe_{a_3} ion was slightly displaced from the heme plane toward the fifth ligand. The Cu_B was 4.5 Å away from Fe_{a_3} and 1.0 Å from the heme normal at Fe_{a_3} position toward the nitrogen atom of the pyrrole with the formyl group. One of the unexpected findings was the absence of a ligand directly bridging the Fe_{a_3} and Cu_B. A bridging ligand has been proposed on the basis of strong antiferromagnetic coupling between the two atoms, a characteristic that was discovered 26 years ago (*15*); other model structures with a bridging ligand have been proposed (*16*). The presence of an amino acid side chain randomly oriented so that the electron density could not be detected by x-ray crystallographic analysis is unlikely because all the amino acid side chains near the dinuclear site have been assigned. However, the presence of water molecules nonspecifically and randomly trapped cannot be excluded.

A typical hydrogen bond is likely to be present between the hydroxyl groups of a tyrosine (Tyr^{244}) and the hydroxyfarnesylethyl side chain of heme a_3 in that the oxygen-oxygen distance is 3.0 Å. Furthermore, the orientation of the phenol plane of Tyr^{244} was perpendicular to the imidazole plane of His^{240}, which liganded to Cu_B. The nitrogen atom of the imidazole of His^{240} was located 3.1 Å above the plane of Tyr^{244}. The system, including the imidazole phenol-hydroxyfarnesylethyl side chain, could facilitate an electron transfer pathway from Fe_{a_3} to Cu_B. A structure that could provide another electron transfer pathway from heme a_3 to Cu_B is the formyl side group at the pyrrole, located 3.0 Å above the imidazole plane of His^{290}, which is a ligand of Cu_B. Although the distance between Fe_{a_3} and Cu_B, as short as 4.5 Å, suggests a facile electron transfer directly between the two metals, multiple electron transfer pathways are still possible for dioxygen reduction. In contrast, these structures may also induce an oxidation state–dependent conformational change to couple O_2 reduction with proton pumping. When Tyr^{244}, which is not bound directly to Cu_B, was replaced by phenylalanine, Cu_B was disrupted (*12*), suggesting some structural role of the amino acid.

Other interesting structures near the heme a_3 and Cu_B site are a hydrogen bond between the imidazole of His^{376} (the fifth ligand of heme a_3) and the peptide carbonyl of Gly^{351}, and a parallel π-π contact between His^{291} of Cu_B ligand and Trp^{236}. The imidazole of a heme a ligand, His^{61}, is linked to a carbonyl oxygen of Gly^{30} with a hydrogen bond. No close contact with the formyl group of heme a is detectable.

Structure of Cu_A. The Cu_A site in subunit II consists of six ligands, two cysteines (Cys^{196} and Cys^{200}), two histidines (His^{161} and His^{204}), a methionine (Met^{207}), and a peptide carbonyl of a glutamate (Glu^{198}) (Fig. 5). All these ligands, except for the peptide carbonyl, have been proposed as a result of mutagenesis experiments (*17*). The anomalous Fourier map at the central metal site exhibited a single peak (Fig. 1), which suggested a single metal, although both the peak heights in the Fourier and the anomalous Fourier maps, respectively, were too high to be attributable to a single copper atom (Table 1). The arrangement of these six ligands, determined from the electron density distribution near this site, does not provide any reasonable position for a single copper atom, but is fully consistent with a dinuclear copper center, as follows. Two copper atoms are bridged by two sulfur atoms of Cys^{196} and Cys^{200}, placing the four atoms on the same plane with the interatomic distances of 2.7 Å (Cu–Cu), and 3.8 Å (Sγ–Sγ). One of the copper atoms is coordinated by the imidazole nitrogen of His^{161} and the methionine sulfur of Met^{207}, forming a tetrahedral coordination including the two cysteine sulfur atoms. Coordination of the other copper is also tetrahe-

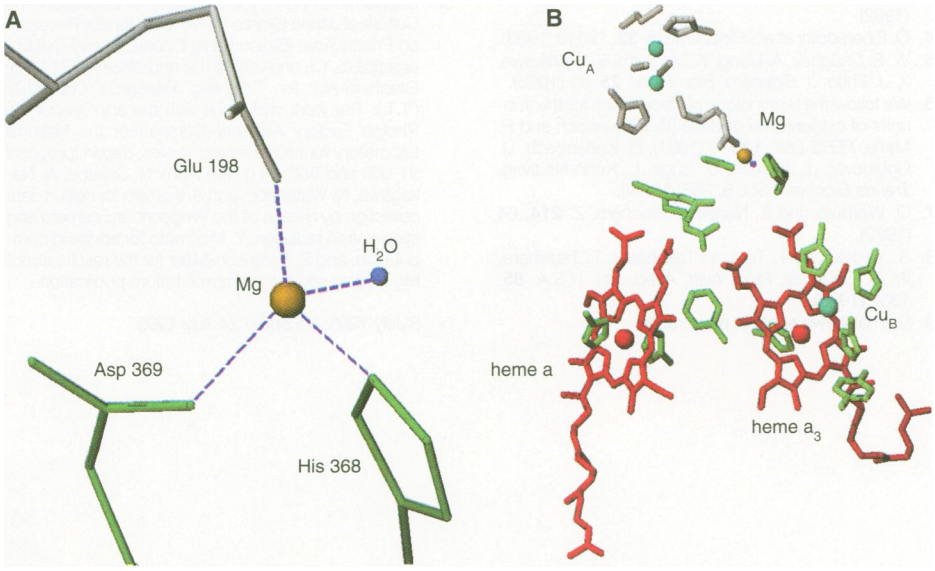

Fig. 6. The magnesium site and its relative orientation to other metal centers. (**A**) Coordination of magnesium. Green and light gray colors denote amino acid residues of subunits I and III, respectively. Dark orange and blue balls are at the positions of magnesium atom and oxygen atom of water, respectively. Blue broken lines are coordination bonds forming a distorted tetrahedron. (**B**) Location of the magnesium site and other active centers. Belonging of amino acids is shown with the same colors as in (A). Positions of iron, copper, magnesium, and oxygen of water are indicated with red, blue, dark orange, and dark blue balls, respectively.

dral, including the imidazole nitrogen (His^{204}) and the peptide carbonyl (Glu^{198}). The geometry is similar to that of a [2Fe-2S]–type iron-sulfur center (*18*), in which the Fe ions and inorganic sulfur atoms are replaced with Cu ions and cysteine sulfur atoms, respectively. Both dinuclear centers stabilize a one-electron delocalized oxidation state, that is, $[Fe^{2.5+}\text{---}Fe^{2.5+}]$ in the reduced form of [2Fe-2S] center and $[Cu^{1.5+}\text{---}Cu^{1.5+}]$ in the oxidized state of [2Cu-2Sγ] center of Cu_A site. Recently, a dinuclear Cu center for Cu_A has been proposed in analogy to that of the copper enzyme N_2O reductase for which various structures not fully consistent with our structure have been suggested (*19*).

Structures of zinc and magnesium sites. Tetrahedral coordination was detectable for the zinc site where four cysteines (Cys^{60}, Cys^{62}, Cys^{82}, and Cys^{85}) in subunit Vb are coordinated by the central atom (Fig. 1C). The polypeptide fragment from Cys^{60} to Cys^{82} shows a zinc finger motif. However, the fragment does not form any protrusion from a globular core of the protein subunit, contrary to the typical zinc finger structure which interacts with a double-stranded DNA (*20*).

The electron density distribution of the enzyme crystals showed several other coordination structures, each with a central atom, that did not show any anomalous scattering for the x-rays at 1.0 Å. One of them involved an aspartate (Asp^{369}) and His^{368} in subunit I, Glu^{198} in subunit II, and an oxygen atom of water as the ligands in a distorted tetrahedral coordination (Fig. 6A). In agreement, Ferguson-Miller *et al.* discovered that His^{411} and Asp^{412} of *Rhodobacter sphaeroides*, which corresponds to His^{368} and Asp^{369} in beef heart enzyme, respectively, are essential for manganese binding to the enzyme at a site for which magnesium competes (*21*). Furthermore, electron density at this site is at a level reasonable for a magnesium atom. Thus, this site is highly likely to be a magnesium site. The magnesium site was found near (approximately 6 Å away from) two adjacent arginine residues (Arg^{438} and Arg^{439}) that faced diagonally to two propionic acid side groups of pyrroles of both hemes to form a tetrahedron involving two positively charged and two negatively charged groups. One of the ligands of the magnesium site, Glu^{198} of subunit II, was also coordinated to Cu_A at the peptide carbonyl, suggesting an oxidation state–linked conformational change which controls the electron transfer pathways between Cu_A and Fe_a and between Fe_a and Fe_{a_3} via the Arg–propionic acid system as stated above. A structural role of the magnesium for stabilizing the Cu_A site is also possible in that mutagenesis data suggest that Glu^{198} is required for forming the Cu_A site (*17*). The magnesium site is located on the hypotenuse of a right-angled triangle including Fe_a, Fe_{a_3}, and Cu_A with Fe_{a_3}–Cu_A as the hypotenuse (Fig. 6B). The presence of zinc and magnesium in equimolar amount of heme a_3 has been reported from several laboratories (*8*, *22*). However, the roles of these metals have not been clear. Our data clearly indicate the presence of intrinsic zinc and magnesium.

The above metal site structures are not completely consistent with the structures obtained from EXAFS. The inconsistency may be due to differences in the model used for the analysis of EXAFS data (*23*). The active site structures obtained here, although they resolve many controversies, require further refinement for the elucidation of the reaction mechanism of this enzyme.

REFERENCES AND NOTES

1. R. A. Capaldi, *Annu. Rev. Biochem.* **59**, 569 (1990).
2. B. G. Malmström, *Chem. Rev.* **90**, 1247 (1990).
3. G. T. Babcock and M. Wikström, *Nature* **356**, 301 (1992).
4. Ó. Einersdottir *et al.*, *Biochemistry* **32**, 12013 (1993).
5. W. S. Caughey, A. Dong, V. Sampath, S. Yoshikawa, X.-J. Zhao, *J. Bioenerg. Biomembr.* **25**, 81 (1993).
6. We follow the terminology of Kadenbach for the subunits of cytochrome oxidase [B. Kadenbach and P. Merle, *FEBS Lett.* **135**, 1 (1981); B. Kadenbach, U. Ungibaver, J. Jaraush, U. Büge, L. Kuhn-Neutwig, *Trends Biochem. Sci.* **8**, 398 (1983)].
7. O. Warburg and E. Negelein, *Biochem. Z.* **214**, 64 (1929).
8. S. Yoshikawa, T. Tera, Y. Takahashi, T. Tsukihara, W. S. Caughey, *Proc. Natl. Acad. Sci. U.S.A.* **85**, 1354 (1988).
9. S. Yoshikawa *et al.*, in preparation.
10. S. Yoshikawa, M. G. Choc, M. C. O'Tool, W. S. Caughey, *J. Biol. Chem.* **252**, 5498 (1977).
11. G. M. Baker, M. Noguchi, G. Palmer, *ibid.* **262**, 595 (1987).
12. J. P. Hosler *et al.*, *J. Bioenerg. Biomembr.* **25**, 121 (1993); B. L. Trumpower and R. B. Gennis, *Annu. Rev. Biochem.* **63**, 675 (1994).
13. B. C. Hill, *J. Biol. Chem.* **266**, 2219 (1991).
14. W. S. Caughey *et al.*, *ibid.* **250**, 7602 (1969).
15. B. F. Van Gelder and H. Beinert, *Biochim. Biophys. Acta* **189**, 1 (1969).
16. S. C. Lee and R. H. Holm, *J. Am. Chem. Soc.* **115**, 5833 (1993); A. Nanthakuman *et al.*, *ibid.*, 8513; G. Palmer, G. T. Babcock, L. E. Vickery, *Proc. Natl. Acad. Sci. U.S.A.* **73**, 2206 (1976); C. H. A. Seiter and S. G. Angels, *ibid.* **77**, 1806 (1980).
17. M. Kelly *et al.*, *J. Biol. Chem.* **268**, 16781 (1993).
18. T. Tsukihara *et al.*, *J. Biochem.* **90**, 1763 (1981).
19. P. M. H. Kroneck, W. A. Antholine, J. Riester, W. G. Zumft, *FEBS Lett.* **247**, 70 (1988); B. G. Malmström and R. Aasa, *ibid.* **325**, 49 (1993); N. J. Blackburn, M. E. Barr, W. H. Woodruff, J. van der Oost, S. de Vries, *Biochemistry* **33**, 10401 (1994); H. Bertagnolli and W. Kaim, *Angew. Chem. Int. Ed. Engl.* **34**, 771 (1995).
20. T. Härd *et al.*, *Science* **249**, 157 (1990).
21. J. P. Hosler, M. P. Espe, Y. Zhen, G. T. Babcock, S. Ferguson-Miller, *Biochemistry* **34**, 7586 (1995); M. P. Espe, J. P. Hosler, S. Ferguson-Miller, G. T. Babcock, J. McCracken, *ibid.*, p. 7593.
22. Ó. Einersdottir and W. S. Caughey, *Biochim. Biophys. Res. Commun.* **129**, 840 (1985); G. C. M. Steffens, T. Souliname, G. Wolf, G. Buse, *Eur. J. Biochem.* **213**, 1149 (1993); M. Öblad *et al.*, *Biochim. Biophys. Acta* **975**, 267 (1989).
23. R. A. Scott, *Annu. Rev. Biophys. Biophys. Chem.* **18**, 137 (1989).
24. N. Sakabe, *J. Appl. Cryst.* **16**, 542 (1983).
25. Z. Otwinowski, DENZO, "A film processing program for macromolecular crystallography" (Yale University, New Haven, CT, 1985).
26. ———, MLPHARE *CCP4 Proc.*, p. 80 (1991) (Daresbury Laboratory, Warrington, UK).
27. D. W. Green, V. M. Ingram, M. F. Perutz, *Proc. R. Soc. London Ser. A* **225**, 287 (1954).
28. B. C. Wang, *Methods Enzymol.* **115**, 90 (1985).
29. A. T. Brunger, *Nature* **355**, 472 (1992).
30. G. Bricogne, *Acta Crystallogr. A* **30**, 395 (1974); *ibid.* **32**, 832 (1974).
31. T. A. Jones, *J. Appl. Cryst.* **11**, 268 (1978).

32. Supported in part by the Ministry of Education and Culture of Japan Grants-in-Aid for Scientific Research on Priority Area [Bioinorganic Chemistry and Cell Energetics (S.Y.), and 06276102 and 05244102 (T.T.)]; Grants-in-Aid for Scientific Research 06558102 (T.T.). The work was done with the approval of the Photon Factory Advisory Committee, the National Laboratory for High Energy Physics, Japan (proposal 91-050 and 94G-041). We thank N. Sakabe, A. Nakagawa, N. Watanabe, and S. Ikemizu for help in data collection by means of the Weissenberg camera and synchrotron radiation, Y. Morimoto for advise in computation, and S. Ferguson-Miller for the results about Mg binding site in the enzyme before publication.

3 July 1995; accepted 24 July 1995